Induced Drag Based on Leading Edge Suction for a Helicopter in Forward Flight

Chenhao Li,* David Poling,† and David Wu‡
Boeing Helicopter Company, Philadelphia, Pennsylvania

Estimating induced drag for a helicopter in forward flight is a three-dimensional, unsteady aerodynamic problem complicated by fluid compressibility and wake geometry. Based on an acceleration potential approach, the chordwise velocity and the derivative $\partial\Phi/\partial t$ of the velocity potential at the leading edge of a thin rotor blade in subsonic flow were re-examined in this paper to assess unsteady and compressibility effects on the induced drag using a leading-edge suction model. The chordwise velocity was shown to have a singular and a continuous component. The $\partial\Phi/\partial t$ was shown to be continuous and hence does not contribute to induced drag. The induced drag calculated from the leading-edge suction model and the more traditional model to be referred to as the induced angle model were compared to quantify the differences in the two approaches. The results show that variations can be significant. While these variations cannot substantiate the validity of either approach, it is clear that the leading edge suction model is simpler to apply with fewer assumptions.

Nomenclature

A_∞ = slope of curve of section lift against angle of attack
a_∞ = speed of sound in the undisturbed air
b = defined in Eq. (16) as $(1-M^2)$
c = semichord
D_i = induced drag based on induced angle method
D_ℓ = induced drag based on leading-edge suction method
d = distance from (x,y,z) to (ξ,η,ζ) or $\sqrt{[x-\xi(T)]^2+[y-\eta(T)]^2+[z-\zeta(T)]^2}$
f = defined in Eq. (22)
H = continuous function of velocity
K = constant defined in Eq. (11) as $\dfrac{1}{4\pi\rho_\infty}$
M = Mach number $\left(\dfrac{U_1}{a_\infty}\right)$
ℓ,m,n = direction cosines of the blade and its wake surface
Q_m = defined in Eq. (11) as $-(x-\xi)\dfrac{d\xi}{dT}-(y-\eta)\dfrac{d\eta}{dT}-(z-\zeta)\dfrac{d\zeta}{dT}$
R = defined in Eq. (16) as $[(x_1-\xi_1+U_1t)^2+b^2(y_1-\eta_1)^2+b^2(z_1-\zeta_1)^2]^{1/2}$
S = leading-edge suction
t = defined in Eq. (11) as $\left(t-\dfrac{d}{a_\infty}\right)$
U_1 = local section velocity of the blade element $(\eta_1\Omega+V_\infty\sin\phi)$
u = chordwise velocity on the thin blade $=u_1+u_2$
V_∞ = forward velocity
v = spanwise velocity on the thin blade
W = inflow or the normal velocity induced by the wake
Y = sectional lift
x,y,z = coordinate at which velocity is calculated
α = blade element angle of attack
ΔP = pressure difference
ξ,η,ζ = coordinates of doublet path
ρ,Θ_0 = cylindrical coordinates of the doublet on the blade
ρ_∞ = undisturbed air density
τ = time the doublet emits a disturbance defined in Eq. (16) as $\left[t+(x_1-\xi_1)\dfrac{U_1}{a_\infty^2}-\dfrac{R}{a_\infty}\right]/b^2$
ϕ = azimuth angle measured from downward position in the direction of rotation
Φ = velocity potential for the entire rotor
Φ' = velocity potential for a moving doublet
ψ = acceleration potential
Ω = rotor speed
ω = defined in Eq. (18) as $\left(\dfrac{n\Omega}{b^2U_1}\right)$
$\dfrac{\partial}{\partial\eta_0}$ = normal derivative of the surface of the doublet
ξ_1,η_1 = blade Cartesian coordinates (see Fig. 2)

Introduction

IT is very important to calculate drag in order to estimate the power required by a helicopter. Induced drag is the largest component of drag for a helicopter in hover or in low-speed forward flight. In high-speed forward flight, induced drag produces torsional moments when there is out-of-plane bending of the blades. The torsional deflection caused by the drag contributes to the change in the angle of attack of the blade element which affects airloads and pitch link loads.

We begin by presenting the less complicated derivation of induced drag for fixed-wing aircraft. We then extend the discussion to helicopters. There are two successful models for estimating the induced drag of fixed-wing aircraft. The traditional model and the induced angle model requires tilting the lift to an induced angle of W/V_∞.[1] In order to estimate induced drag from a lifting surface theory using this model, the distribution of normal induced velocity W over the whole chord must be calculated. The second model requires calculating the leading-edge suction and subtracting it from the backward component of the aerodynamic force normal to the chord.[2,3] In this manner the 2-D concept of leading-edge suction is extended to 3-D assuming that it depends only on the character of the chordwise velocity at the leading edge. This model neglects the effects of airfoil thickness, which does not influence induced drag. Only the chordwise velocity at a single point is necessary for this analysis.

For a helicopter in forward flight, the traditional approach for estimating induced drag[4] is to first calculate the normal velocity W, which is induced by the wake. The lift is then tilted

Received May 22, 1987; revision received April 1989.

*Visiting Scientist, Aeromechanics.
†Technical Specialist, Aeromechanics. Member AIAA.
‡Engineer, Systems Analysis.

to an induced angle of W/U_1. This is an extension of the traditional fixed-wing-induced angle model. An alternative approach for estimating induced drag of a helicopter rotor is to extend the 3-D fixed-wing, leading-edge suction model to a rotor.

The Boeing Helicopter Company has been developing a new method based on the leading-edge suction model to calculate induced drag and performance of a helicopter rotor in hover. By using an acceleration potential technique with a prescribed wake, which accounts for compressibility effects, the lift distribution is obtained from the solution of an integral equation.[7] Figure 1 is an example of the predicted rotor performance showing good correlation with measurements.

To date, the application of the leading-edge suction model has been limited to helicopters in hover.[5] This paper extends the leading-edge suction model to helicopters in forward flight by examining two parameters, specifically u and $\partial\Phi/\partial t$ and also to account for unsteady and compressibility effects. Though the approach may be applicable in supersonic flows, the current discussion will be limited to subsonic flows.

Preliminary Comparison of Approaches to Estimate Induced Drag

The two approaches will be initially compared using lifting-line theory before extending the comparison to lifting-surface theory. For fixed-wing aircraft flying in an incompressible steady flowfield,

$$\Delta P(x,y) = A(y)\left[\frac{(c-x)}{(c+x)}\right]^{1/2} \tag{1}$$

where the lift per length is

$$Y(y) = A(y)c\pi \tag{2}$$

By extending the 2-D airfoil relationship between u and the leading-edge suction to 3-D, the leading-edge suction S and induced drag D_ℓ can be written as

$$S = \pi\rho_\infty\left[A(y)\frac{\sqrt{2c}}{2\rho_\infty V_\infty}\right]^2 \tag{3}$$

$$D_\ell = Y(y)\alpha - S \tag{4}$$

The lift-per-unit span can be written as

$$Y(y) = \tfrac{1}{2}[\rho_\infty V_\infty^2(2c)A_\infty(\alpha - W/V_\infty)] \tag{5}$$

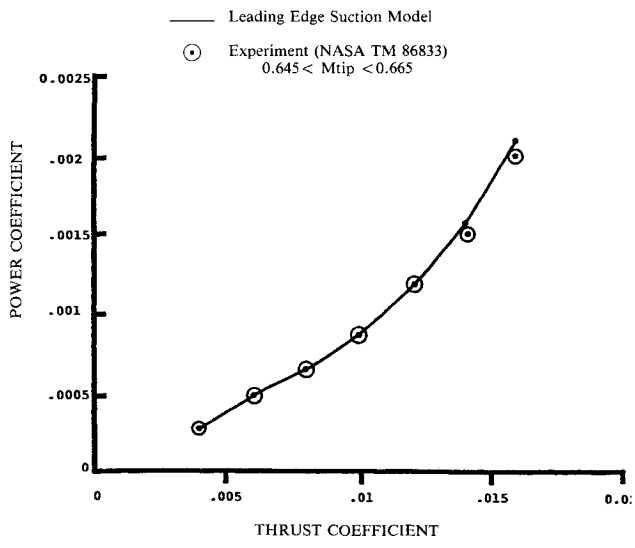

Fig. 1 Variation in power with thrust coefficient. Comparisons with experiment and predictions from the leading-edge suction model. (Experiments were performed at the NASA Ames Outdoor Aerodynamic Research Facility using the XV-15, three-bladed, full-scale rotor configuration with a NACA 64-series airfoil.)

and based on the induced angle model, the induced drag D_i is

$$D_i = Y(y)\frac{W}{V_\infty} \tag{6}$$

From these equations, it can be shown that $D_i = D_\ell$ if $A_\infty = 2\pi$, the theoretical value for steady flow. This comparison shows that there is no difference in the two approaches for fixed-wing aircraft in steady flows based on lifting-line theory. For fixed-wing aircraft not complicated by curved wakes, this result can be extended to compressible flow using the Prandtl-Glauert compressibility factor.

Lifting-line theory is not adequate in describing helicopters in forward flight because the flowfield is unsteady; there are multiblade interference effects, and the wake is curved. It is therefore unreasonable to expect the estimated induced drag based on the induced angle model to be the same as that obtained from the leading-edge suction model. Furthermore, the $\partial\Phi/\partial t$ contribution to induced drag is often ignored in the induced angle model.

In order to estimate induced drag using the leading-edge suction model, an expression for the chordwise velocity must be obtained. By constructing a small circle around the leading edge in a plane perpendicular to the span of the blade, it can be deduced that the contribution of the continuous terms to the resultant force from the pressure acting on the circle, as given by the unsteady Bernoulli equation

$$\frac{\Delta P}{\rho_\infty} + \frac{u^2}{2} + \frac{\partial\Phi}{\partial t} = \text{const} \tag{7}$$

goes to zero when the circle shrinks to the leading edge. Therefore, it is only the singular portion of the chordwise velocity and the unsteady term $\partial\Phi/\partial t$ which contribute to the induced drag. These terms will be examined separately. For a fixed-wing aircraft and for a small perturbation of the flow

$$\Delta P = \rho_\infty\left[V_\infty(U_u - U_\ell) + \tfrac{1}{2}(U_u^2 - U_\ell^2)\right] = 2\rho_\infty V_\infty u \tag{8}$$

where the subscripts u and ℓ mean upper and lower surface, respectively. Hence $u = \Delta P/2\rho_\infty V_\infty$. At the leading edge, u is singular as well as ΔP.

The comparable equation for a helicopter in forward flight is[6]

$$\Delta P = -\rho_\infty\left[\partial\Phi/\partial t + (V_\infty + \Omega y)u - \Omega x v + W\partial\Phi/\partial z\right] \tag{9}$$

The relationship between u and ΔP cannot be derived from Eq. (9) directly. However, the desired relationship can be derived from an analysis of pressure doublets moving with the blade and wake.

Acceleration Potential and Velocity Potential

For a small perturbation of an undisturbed medium, the governing equation in a fixed reference frame for the acceleration potential Ψ is the wave equation.[7] Thus,

$$\frac{\partial^2\Psi}{\partial x^2} + \frac{\partial^2\Psi}{\partial y^2} + \frac{\partial^2\Psi}{\partial x^2} - \frac{1}{a_\infty^2}\left(\frac{\partial^2\Psi}{\partial t^2}\right) = 0 \tag{10}$$

The acceleration potential for a moving doublet is expressed as

$$\Psi(x,y,z,t) = K\frac{\partial}{\partial\eta_0}\left[\frac{\Delta P(\xi_1,\eta_1,T)}{d + Qm/a_\infty}\right] \tag{11}$$

Clearly the curved wake compressibility effects do not take the form of the Prandtl-Glauert compressibility factor. The clear advantage of using the acceleration potential technique is to properly account for the curved wake effects in a compres-

sible medium. For a small perturbation

$$\Psi = \partial\Phi/\partial t = \mathrm{d}\Phi/\mathrm{d}t \tag{12}$$

Assuming $\Phi \to 0$ as $t \to -\infty$, which is the theoretically correct lower limit for Eq. (12)[8]

$$\Phi = \int_{-\infty}^{t} \Psi \mathrm{d}t$$

The velocity potential of a moving doublet Φ' at $t=0$ is

$$\Phi' = K\int_{-\infty}^{0} \frac{\partial}{\partial\eta_0}\left[\frac{\Delta P(\xi_1,\eta_1,T)}{d+Qm/a_\infty}\right]\mathrm{d}t$$

and the contribution of all the doublets to the velocity potential Φ at $t=0$ is written as

$$\Phi = K\int\int \mathrm{d}\xi_1\,\mathrm{d}\eta_1 \int_{-\infty}^{0} \frac{\partial}{\partial\eta_0}\left[\frac{\Delta P(\xi_1,\eta_1,T)}{d+Qm/a_\infty}\right]\mathrm{d}t \tag{13}$$

Continuity of Chordwise Velocity and $\partial\Phi/\partial t$

The chordwise velocity along the blade is $u = \lim_{z\to 0} \partial\Phi/\partial x$. To separate the multiblade interference effects, the chordwise velocity is separated into two components u_1 and u_2. The component u_2 is the contribution from the reference blade, and u_1 is the contribution from all the other blades and wakes. Since the flowfield generated by a doublet is singular only at the location of the doublet, u_1 must be continuous.

The chordwise velocity u_2 at $(x,y,0)$ contributed by a doublet moving with the reference blade is singular when the doublet passes through the point $(x,y,0)$. This singularity disappears after the double integral extending over the blade is performed. Therefore the limit $z\to 0$ must not be taken inside the double integral in Eq. (13), but the order of the mathematical operators may be changed.

The velocity at $t=0$ contributed by the doublet moving with the reference blade is

$$\Phi_2 = K\int\int \mathrm{d}\xi_1\,\mathrm{d}\eta_1 \int_{-\tau_{0_1}}^{0} \frac{\partial}{\partial\zeta}\left[\frac{\Delta P(\xi_1,\eta_1,T)}{d+Qm/a_\infty}\right]\Bigg|_{t=0}\mathrm{d}t \tag{14}$$

where τ_{0_1} is the time required by the doublet to move from the point at which the doublet is located at $t=0$ to the corresponding trailing edge. From Fig. 2, the chordwise velocity at $t=0$ is

$$u_2 = \lim_{z\to 0}\frac{\partial\Phi_2}{\partial x_1}\Big|_{t=0} = K\lim_{z\to 0}\frac{\partial}{\partial x_1}\int\int \mathrm{d}\xi_1\,\mathrm{d}\eta_1\int_{\tau_{0_1}}^{0}\frac{\partial}{\partial\zeta}$$

$$\times\left[\frac{\Delta P(\xi_1,\eta_1,T)}{d+Qm/a_\infty}\right]\Bigg|_{\zeta=0}\mathrm{d}t \tag{15}$$

Linearizing the doublet's path yields

$$u_2 = K\lim_{z\to 0}\frac{\partial}{\partial x_1}\int\int \mathrm{d}\xi_1\,\mathrm{d}\eta_1\left(\int_{-\infty}^{0} - \int_{-\infty}^{-\tau_{0_1}}\right)\frac{\partial}{\partial\zeta}$$

$$\times\left[\frac{\Delta P(\xi_1,\eta_1,T)}{d+Qm/a_\infty}\right]\Big|_{\zeta=0}dt \tag{16}$$

The contribution to u_2 from the integral $\int_{-\infty}^{-\tau_{0_1}}$ is continuous. Letting $u_2 = u_2' + H$, where H represents the continuous portion and expanding ΔP in a Fourier series in time yields

$$u_2' = K\lim_{z\to 0}\int\int \mathrm{d}\xi_1\,\mathrm{d}\eta_1\frac{\partial}{\partial x_1}\frac{\partial}{\partial\zeta}\sum_{n=0}^{\infty}\Delta P_n(\xi_1,\eta_1)\int_{-\infty}^{0}$$

$$\times\frac{\exp(\mathrm{i}n\Omega\tau)}{R}\,\mathrm{d}t\Big|_{\zeta=0} \tag{17}$$

The innermost integral is uniformly convergent and thus the order of the differential operator $\partial^2/\partial x_1\partial\zeta$ and the summation operator Σ can be interchanged. The innermost integral in Eq. (17) was fully analyzed by Watkins, Runyan, and Woolston,[9] and it may be shown that the singularity of the innermost integral occurs at

$$\frac{\partial^2}{\partial x_1\partial\zeta}\int_{-\infty}^{0}\frac{\exp(\mathrm{i}n\Omega\tau)}{R}\,\mathrm{d}t\Big|_{\zeta=0} = \frac{b^2 z}{u_1}$$

$$\times\frac{\exp\left[\mathrm{i}\omega(M^2(x_1-\xi_1) - M\sqrt{(x_1-\xi_1)^2+b^2(y-\eta)^2+b^2z^2}\right]}{\left(\sqrt{(x_1-\xi_1)^2+b^2(y-\eta)^2+(b^2z^2)}\right)^3} \tag{18}$$

By introducing the transformation $x-\xi = r\cos\Theta$, $y-\eta = r\sin\Theta/b$, the singular term in u_2 becomes

$$u_2' = \frac{K}{U_1}\lim_{z\to 0}\lim_{\epsilon\to 0}\int_0^{2\pi} d\Theta\int_\epsilon^R \frac{bzr\,\mathrm{d}r}{(\sqrt{r^2+b^2z^2})^3}\cdot\sum_{\ell=0}^{\infty}\sum_{n=0}^{\infty}\frac{(-1)^\ell}{\ell!}$$

$$\left(r\cos\Theta\frac{d}{\mathrm{d}\xi} + r\sin\Theta\frac{d}{\mathrm{d}\eta}\right)^\ell \Delta P(\xi,\eta)\,|_{(x,y)}\sum_{m=0}^{\infty}$$

$$\frac{\left[\mathrm{i}\omega(M^2 r\cos\Theta - M\sqrt{r^2+b^2z^2})\right]^m}{m!} \tag{19}$$

For $\ell=0$ and $m=0$ in Eq. (19),

$$\lim_{z\to 0}\lim_{\epsilon\to 0}\int_0^{2\pi} d\Theta\int_\epsilon^R \frac{bzr\,\mathrm{d}r}{(\sqrt{r^2+b^2z^2})^3} = \pm 2\pi$$

for $\ell>0$ and $m>0$ the integral in Eq. (19) is zero due to the higher power of r and/or $\sqrt{r^2+b^2z^2}$. Therefore, $u_2 = \Delta P/2\rho_\infty U_1 +$ continuous terms and

$$u = u_1 + u_2 = \frac{\Delta p}{2\rho_\infty U_1} + H \tag{20}$$

The continuity of $\partial\Phi/\partial t$ can be shown using an argument similar to that for the chordwise velocity.

Summary and Quantitative Comparison

Using the acceleration potential technique which accounts for the effects of a curved wake and compressibility, it has been shown that the chordwise velocity in the neighborhood of the leading edge is $u = \Delta P/2\rho_\infty U_1 + H$ and that $\partial\Phi/\partial t$ and H are continuous. By combining Eqs. (1) and (20), the 3-D, fixed-wing relationship between u and the leading-edge suction

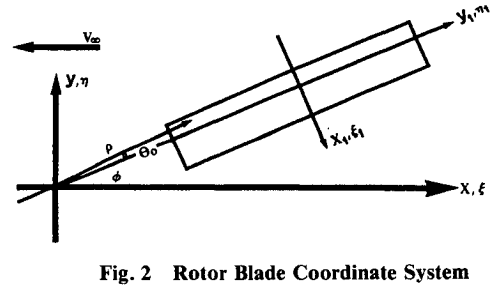

Fig. 2 Rotor Blade Coordinate System

Table 1 Value of f for Varying Normalized Radial (r/R) Positions

	First Rotor at 0.2 Advance Ratio[3,10,12]						
r/R	0.4	0.5	0.6	0.7	0.8	0.9	1.0
f	0.696	0.691	0.703	0.697	0.692	0.790	0.838
	Second Rotor at 0.38 Advance Ratio[12]						
r/R		0.26		0.39		0.52	0.64
f		0.978		0.956		0.863	0.872

may be extended to a helicopter rotor in forward flight

$$S = \pi\rho_\infty b\left(A_0 \frac{\sqrt{2c}}{2\rho_\infty U_1}\right)^2 \tag{21}$$

In order to quantify the difference between the traditional induced angle model and leading-edge suction model for estimating induced drag, the following function is defined

$$f = \frac{y\dfrac{W}{U_1}}{y\alpha - S} \tag{22}$$

Table 1 shows the values of the function f for two rotors[12] at different advance ratios. The advance ratio for the first rotor is 0.2. The lift distribution was modified by using the 2-D Theodorsen function. The advance ratio for the second rotor is 0.38. The values of the function f were obtained assuming the near wakes and middle wakes produced a uniform downwash.

As is clear from the values in Table 1, the induced drag calculated from the traditional induced angle model ranges from 69–84% of the induced drag calculated from the leading-edge suction model at an advance ratio of 0.2 and 86–98% at an advance ratio of 0.38. In other words, the induced angle model consistently underestimates the induced drag. This might result from neglecting the contribution of $\partial\Phi/\partial t$. This problem does not exist in the leading-edge suction model because the contribution of $\partial\Phi/\partial t$ to the induced drag is properly accounted for.

Conclusion

By extending the leading-edge suction model to a helicopter rotor in forward flight, two contributors to induced drag which have largely been neglected in the traditional induced angle model can be included. First, the contribution of induced drag from the nonzero term $\partial\Phi/\partial t$ in the induced angle model is shown to produce a zero contribution to induced drag in the leading-edge suction model. Second, the Prandtl-Glauert compressibility factor, which should not apply to helicopters in forward flight due to the motion of the rotor relative to the airstream, is properly considered using an acceleration potential technique. A better understanding of the induced drag was obtained by deriving quantifiable expressions for the chordwise velocity u and the time rate of change of the velocity potential $\partial\Phi/\partial t$. A comparison of the present model with the traditional induced angle model shows the traditional induced angle model underestimates the induced drag by as much as 31%. While these differences cannot substantiate the validity of either approach, it is clear that the leading-edge suction model is based on fewer assumptions and simpler to apply.

References

[1]Milne Thomsen, L. M., "Theoretical Aerodynamics," 4th ed., Dover, New York, 1973, pp. 181–232.

[2]Sears, W. R., "General Theory of High Speed Aerodynamics," Vol. 6D, Princeton University Press, Princeton, NJ, 1954, Chap. 3, pp. 218–229.

[3]Wagner, S., "On the Singularity Method of Subsonic Lifting Surface Theory," *Journal of Aircraft,* Vol. 6, 1969, pp. 549–558.

[4]Egolf, T. A. and Landgrebe, A. J., "Helicopter Rotor Wake Geometry and Its Influence in Forward Flight," NASA CR 3726, Dec. 1983.

[5]Kocurek, J. D., Berkowitz, L. F., and Harris, F. D., "Hover Performance Methodology at Bell Helicopter Textron," *Proceedings of the 36th Annual National Forum of the American Helicopter Society,* Wash., DC, May 1980.

[6]Runyan, H. L., "Unsteady Lifting Surface Theory Applied to a Propeller and Helicopter Rotor," Ph.D. Thesis, Loughborough University of Technology, Loughborough, England, July 1983.

[7]Li, C. and Ruan, T., "Study of Pressure Distribution on Rotor Blades with Three-Dimensional Nonsteady Theory of Compressible Fluid," *Acta Aeronautica et Astronautic Sinica,* Vol. 3, No. 2, 1983, pp. 20–28.

[8]Summa, J. H. and Clark, D. K., "A Lifting Surface Method for Hover/Climb Airloads," *Proceedings of the 35th Annual National Forum of the American Helicopter Society,* Wash., DC, May 1979.

[9]Watkins, C. E., Runyan, H. L., and Woolston, D. S., "On the Kernel Function of the Integral Equation Relating the Lift and Downwash Distribution of Oscillating Finite Wings in Subsonic Flow," NACA Rept. 1234, 1955.

[10]Theordorsen, T., "General Theory of Aerodynamic Instability and the Mechanism of Flutter," NACA Rept. 496, May 2, 1934.

[11]Scheiman, J., "A Tabulation of Helicopter Rotor-Blade Differential Pressures, Stresses, and Motion as Measured in Flight," NASA TMX-952, May 1964.

[12]Wang, S. and Xu, Zhi, "A Simplified Method for Predicting Rotor Blade Airloads," *Acta Aeronautica et Aeronautic Sinica,* Vol. 3, No. 2, 1983, pp. 1–17.